International Core Journal of Engineering Volume 7 Issue 8, 2021
ISSN: 2414-1895 DOI: 10.6919/ICJE.202108_7(8).0037

Vibration Characteristics of Inertial Excitation Equipment for Wind Turbine Blade Fatigue Loading Test

Zhongxiang Li*, Xin Zhang

Lianyungang Zhongfu Lianzhong Composites Group Co., Ltd, Jiangsu Lianyungang 222000, China.

Abstract

Aim at fatigue loading test for wind turbine blades, A set of inertial excitation equipment driven by eccentric mass block is designed . Taking a certain type of wind turbine blade as an example, Using the law of conservation of energy and vibration theory derived energy requirements for vibration and the steady-state operating characteristics, and the calculation matched the key parameters of the inertial excitation equipment. Based on the above calculated parameters, the three-dimensional model of inertial excitation equipment was constructed, the finite element method was used to analyze the strength, deformation and fatigue life of pivotal components of the equipment, on this account, the feasibility of the equipment used in fatigue loading test was verified, and it laid the foundation for the smooth progress of the subsequent experiments.

Keywords

Wind Turbine Blade; Fatigue Test; Inertial Excitation Equipment; Vibration Characteristics; Structural Analysis.

1. Introduction

Wind power became the core technology to realize the "beautiful Chinese dream". As the pivotal component of the wind turbine, the quality of the blade determined the healthy development of the wind power industry. The blade subjected to alternating fatigue loads during operation. Fatigue failure was one of the most important failure modes [1-4], therefore, fatigue performance testing became very important.

At present, fatigue testing was mainly carried out by forced loading and inertial resonance at home and abroad [5-6]. Excitation equipment as a key part of the entire fatigue test, its research on fatigue resistance was a link that can not be ignored. This paper researched the vibration characteristics of blade fatigue loading and the start-stop characteristics of the equipment, and completed load characteristic analysis and parameter matching of key components of the excitation equipment, and designed a set of inertial excitation equipment driven by eccentric mass block, and analysed the stress and life of key components of the equipment, and it laid the foundation for the smooth progress of the subsequent experiments.

2. Inertial excitation equipment design

Wind turbine blade inertial excitation equipment included power transmission system, support system, detection control system and safety guarantee system, as was shown in Figure 1. Powertrain system included: power line, frequency converter, deceleration motor, eccentric block; The support system included: blade fixture and bracket; The detection and control system included: laser sensor, PLC and host computer; The safety-guaranteed system included: mechanical safety assurance system and electrical safety assurance system; Mechanical safety assurance system included: safety frames, safety nets and various mechanical anti-loose measures.

ISSN: 2414-1895 DOI: 10.6919/ICJE.202108_7(8).0037

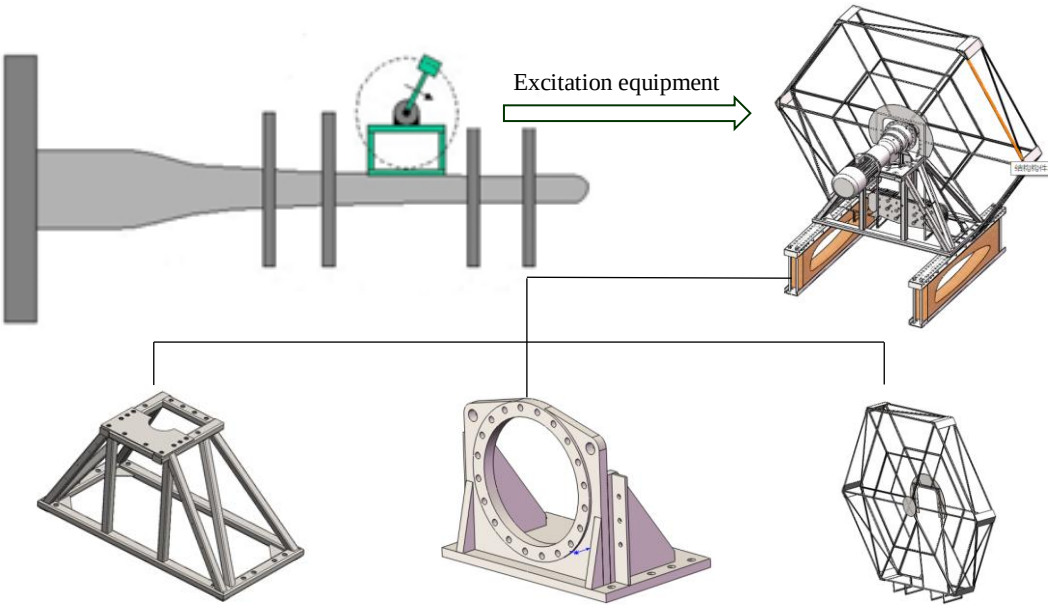

Bracket Coupling Safety net

Fig. 1 General plan of inertial excitation equipment

The loading system worked with the principle of resonance, the geared motor driven the rotating eccentric block to make an approximate sinusoidal rotation in a vertical plane, Centrifugal force acted as an excitation force to work on the blade, by adjusting the size of the eccentric block, the blade reached the amplitude required for the test. Laser range finder monitored blade amplitude changes in real time, PLC controled the inverter to output signal, then adjusted the motor to output speed through the inverter, to make the rotational frequency of the rotating eccentric block real-time as the resonant frequency.

3. Theoretical analysis of inertial excitation

3.1 Theoretical analysis of inertial excitation

The work of the excitation force in one work cycle was:

$$\Delta E = \int_0^T F dx = \int_0^{\frac{2\pi}{\omega}} -mL\omega^2 \cos\ \omega t \times \omega A \sin(\omega t + \Phi)\, dt = \pi mLA\omega^2 \sin\Phi \tag{1}$$

Resonance time $\Phi = -\frac{\pi}{2}$, the loading system did the most work on the blades, is:

$$\Delta E = \pi mLA\omega^2 \tag{2}$$

At the loading point, the blade damping coefficient was c, stiffness coefficient was k, amplitude was A, then in a vibration period, the damping energy consumption ΔW was:

$$\Delta W = \int_0^T cx'dx = \int_0^T cA\omega^2 (\sin(\omega t + \Phi))^2 dt = \pi cA^2\omega = 2\pi kA^2\xi \tag{3}$$

Among $c = \frac{2k\xi}{\omega}$

According to the law of conservation of energy, eccentric block works on the blade was equal to damping dissipation energy, that was, $\Delta E = \Delta W$, resulted in:

$$\pi mLA(2\pi f)^2 = 2\pi kA^2\xi \tag{4}$$

The equivalent mass of the eccentric block can be obtained from the above formula:

$$m = \frac{2\pi kA^2\xi}{4\pi^3 f^2 LA} \tag{5}$$

The measured value of the blade stiffness k was obtained by the modal test method.

ISSN: 2414-1895 DOI: 10.6919/ICJE.202108_7(8).0037

3.2 System startup analysis

Blade motion equation:

$$x(t) = A_0 e^{-\beta t} sin(\omega_d t + \Phi) + A\, cos(\omega t + \Phi) \tag{6}$$

The natural frequency of undamped vibration of the blade was:

$$\omega_0 = \sqrt{\frac{k}{m_e}} \tag{7}$$

The natural frequency of damped vibration of the blade was:

$$\omega_d = \sqrt{\omega_0^2 - \beta^2} = 2\pi f \tag{8}$$

The damping factor was:

$$\beta = \frac{c}{2m_e} = \xi\omega_0 = 2\pi f\xi \tag{9}$$

As can be seen from the above formula, The blade damping factor $\beta =$ ω_0, then:

$$\omega_d \approx \omega_0 = 2\pi f \tag{10}$$

Equivalent mass of the blade at loading point:

$$m_e = \frac{k}{\omega_0^2} = \frac{k}{(2\pi f)^2} \tag{11}$$

The transient response equation of blade was:

$$x(t) = A_0 e^{-\beta t} sin(\omega_d t + \Phi) \tag{12}$$

Vibration reached steady state, that is, the state in which the transient response decayed to zero, Considered $e^{-\beta t} \leq 0.02$ as a sign of entering a steady state, then:

$$t = \frac{n}{f} \geq \frac{ln\,50}{\beta} = \frac{ln\,50}{2\pi f\xi} \tag{13}$$

Before reaching steady state, the number of swinging weeks of the eccentric block n was:

$$n \geq f\,ln\,50 \big/ 2\pi f\xi \tag{14}$$

Motor starting torque:

$$T_s = mgL \tag{15}$$

The starting power of the motor was:

$$p_s = 2\pi f T_S = 2\pi f mgL \tag{16}$$

3.3 Steady state operation analysis

The exciting force of the blade was:

$$F = F_0\, cos\, \omega\, t \tag{17}$$

The steady state equation of motion was:

$$x = A\, cos(\omega t + \Phi) \tag{18}$$

The steady state velocity was:

$$x' = -A\omega\, sin(\omega t + \Phi) \tag{19}$$

The steady state motion acceleration was:

$$x'' = -A\omega^2\, cos(\omega t + \Phi) \tag{20}$$

The resonance frequency was:

$$\omega = \sqrt{\omega_0^2 - 2\beta^2} \tag{21}$$

Phase difference:

$$\Phi = arctan - \frac{\sqrt{\omega_0^2 - 2\beta^2}}{\beta} \tag{22}$$

ISSN: 2414-1895 DOI: 10.6919/ICJE.202108_7(8).0037

Due to the blade $\beta = \omega_0$, the phase angle $\phi = -\frac{\pi}{2}$, approximately believed that the phase angle of the blade vibration lags behind the swing phase angle of the eccentric block $\frac{\pi}{2}$.

In one cycle, The average power applied by the motor was equal to the average power consumed by the blade damping:

$$P_m = \frac{\Delta W}{T} = \Delta W f = 2\pi k A^2 f \xi \tag{23}$$

The average torque was:

$$T_m = \frac{P_m}{2\pi f} = kA^2\xi \tag{24}$$

It was assumed that the power consumed by the blade damping changed in a sinusoidal rule, then the peak power consumed by the motor and the peak power consumed by the blade damping were $\frac{\pi}{\int_0^{\pi} \sin t dt} = \frac{\pi}{2}$ times that of the average power, the peak power was:

$$P_P = \frac{\pi}{2} P_m = \pi^2 k A^2 f \xi \tag{25}$$

Due to blade vibration, the additional torque generated by the eccentric block was:

$$T_a = m x'' L \tag{26}$$

Maximum instantaneous torque at steady state:

$$T_{max} = m(x'' + g)L \tag{27}$$

The motor torque can be checked by the above formula.

Table 1. Parameters of inertial excitation system

Type	Parameter	LZ45.3	LZ48	LZ 40.3	LZ 56.4	LZ59.5
Blade parameter	natural requency	0.47 (0.461)	0.38 (0.384)	0.78	0.57	0.3
	Rigidity k(N/m)	61661	49068	75000	58000	69000
	Damping ratio ξ	0.0205	0.0245	0.02	0.028	0.028
	Amplitude A(m)	1.36 (1.461)	1.63 (1.646)	1.10	1.80	1.8
	Pendulum length L(m)	1.5	1.5	1.5	1.5	1.5
	Equivalent mass of eccentric block m(kg)	263	458	92	304	1097
startup parameter	Starting torque T_s(Nm)	3866	6733	1352	4469	16125
	Starting power P_s(kw)	11.42	16.08	6.63	16.0	30.4
	Steady state revolution n	30	25	31	22	
Steady state parameter	Steady-state mean torque T_m(Nm)	2338	3194	1815	5263	5263
	Steady-state average power P_m(kw)	6.90	7.63	8.90	18.84	9.92
	Steady-state peak power P_p(kw)	10.8	12.0	14.0	30.0	15.6
	Steady state additional torque T_a(Nm)	4679	6384	3646	10528	10523
	Steady maximum torque T_{max}(Nm)	8545	13117	4998	14997	26649
	Steady maximum radial force N	6014	8401	4213	8822	16592

4. Loading characteristics

The fatigue characteristics of the excitation equipment can be described by the maximum stress, the number of stress cycles N, the stress ratio (or cyclic characteristics), this paper was focused on stress and life analysis of key components of the equipment including: eccentric blocks, bushings, pedestals and brackets.

According to the above theoretical analysis, by calculating the load on the critical components outputted result as shown in Figure 2.

ISSN: 2414-1895 DOI: 10.6919/ICJE.202108_7(8).0037

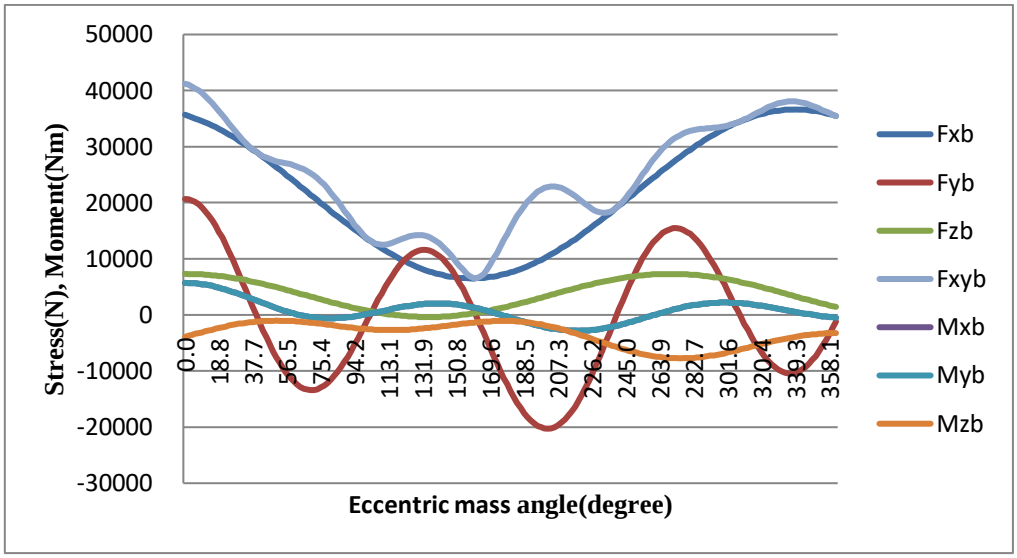

Fig. 2 Load characteristics of components under alternating loads

It can be seen from Table 1 that the key components were affected by the alternating load, it was difficult to get the most dangerous conditions, so it was proposed to solve by finite element method.

The key load that had the greatest influence on the stress of the eccentric block was Fxy:

$$F_{xy\,max} = 22290N \tag{28}$$

$$F_{xy\,min} = 2142N \tag{29}$$

The stress ratio was:

$$r = \frac{F_{xy\,min}}{F_{xy\,max}} = 0.096 \tag{30}$$

The known parameters were as follows: the equivalent arm length of eccentric block was L=1.5m, the blade vibration frequency was f=0.3Hz, the amplitude of the blade at the excitation point was A=1.8m; The quality of eccentric block was mp=1100kg, the equivalent quality of eccentric block was m=1000kg, the quality of reducer was mr=392kg, The quality of motor was mm=349kg, the quality of bell-shaped flange and coupling was mf=200kg quality, the quality of the base of the reducer was mb=160kg, the quality of the scaffold was ms=339kg.

The design life was 50000000 times, the distribution of the safety factor of the eccentric block was shown in Figure 3.

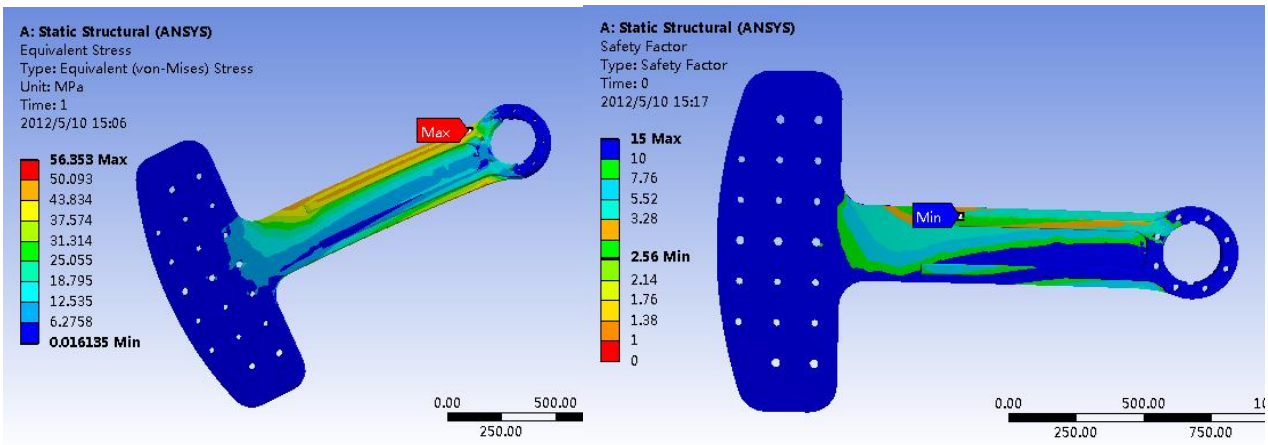

(a) Stress distribution (b) Life analysis

Fig. 3 Fatigue stress distribution and life analysis of eccentric block

ISSN: 2414-1895 DOI: 10.6919/ICJE.202108_7(8).0037

It was calculated that the maximum stress of the eccentric block was 56Mpa, in order to ensure that the part meet the certain strength, various safety factors were introduced at the time of strength check, its value was shown in Table 2.

Table 2. Safety Factor

Safety factor	Value
Material safety factor (static strength and fatigue strength)	$\varsigma_m = 1$
Weld safety factor	$\varsigma_w = 1.5$
Safety factor of parts	$\varsigma_s = 2$

Through the above analysis, the maximum stress σ =75MPa, which was found at the ribbed slab, therefore, the material safety factor was $\xi_m = 1$, the yield limit of material Q345 is σ_s=345Mpa, the allowable stress was:

$$[\sigma] = \frac{\sigma_s}{\varsigma_m \varsigma_s} = 172.5MPa \tag{31}$$

$$\sigma = 75MPa < [\sigma] \tag{32}$$

The minimum fatigue safety factor of eccentric block was 2.5, which met the load requirement.

Spline bushing material selection was 40Cr, when the design life was 50000000 times, the distribution of stress and life of spline were shown in the following figure.

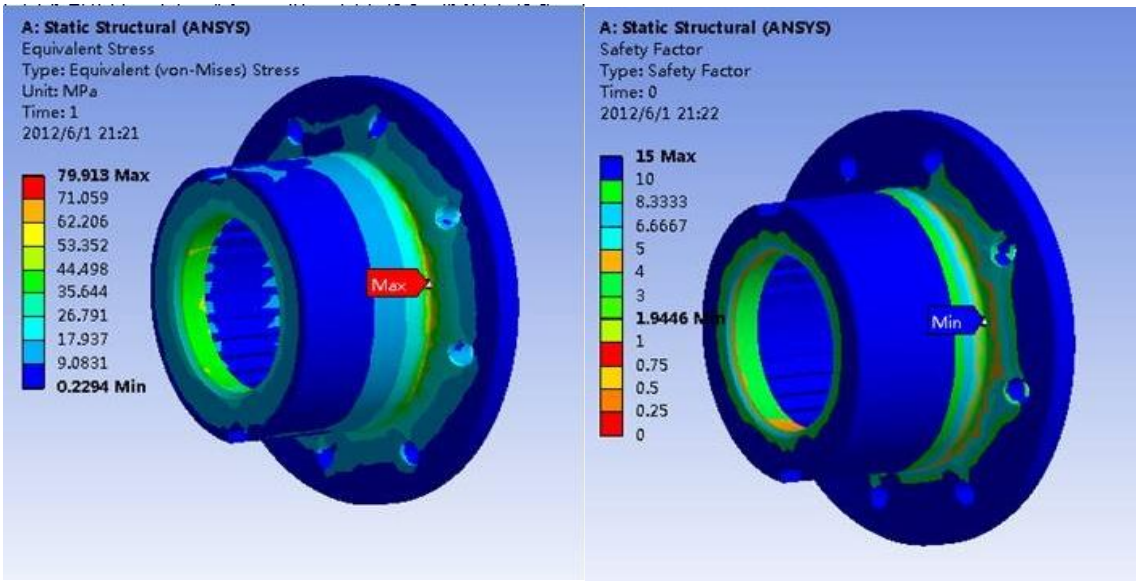

(a) Stress distribution (b) Life analysis

Fig. 4 Analysis of fatigue stress distribution and life of bushing

The maximum stress of the axle sleeve was 80Mpa. Material safety factor was ς_m=1, safety factor of the part was ς_s=2, the yield limit of material 40Cr was σ_s=490Mpa, the allowable stress was:

$$[\sigma] = \frac{\sigma_s}{\varsigma_m \varsigma_s} = 245MPa \tag{33}$$

$$\sigma = 80MPa < [\sigma] \tag{34}$$

The minimum fatigue safety factor of spline shaft sleeve was 1.9, the actual material used for spline shaft bushing was 40Cr, and its yield limit was 490MPa, which was greater than the yield limit of Q345, so the fatigue safety factor of spline shaft bushing was greater than 1.9.

When the design life of base was 50000000 times, the stress and life distribution of the base were shown in the figure below.

ISSN: 2414-1895 DOI: 10.6919/ICJE.202108_7(8).0037

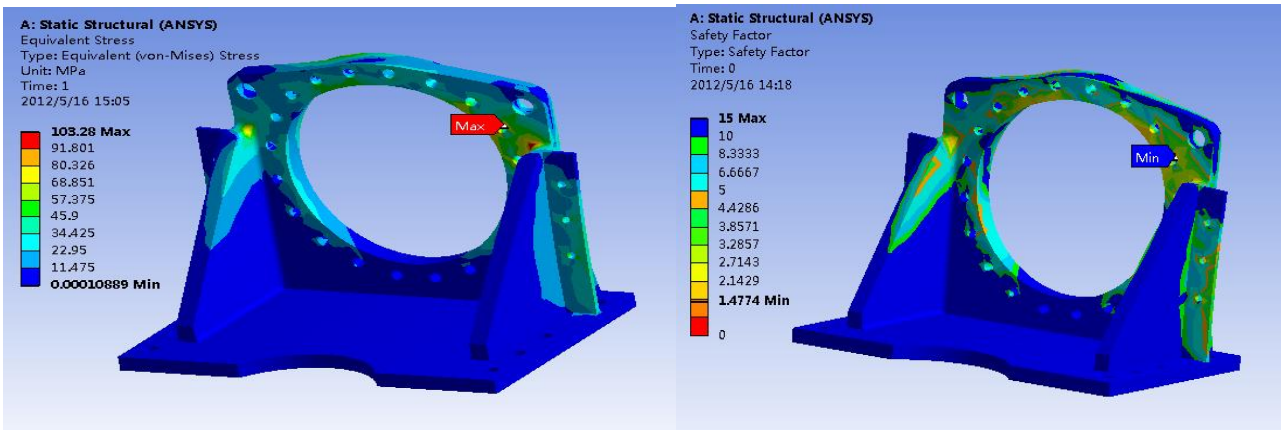

(a) Stress distribution (a) Life analysis

Fig. 5 Fatigue stress distribution and life analysis of axle sleeve

The maximum stress of the pedestal was calculated to be 103 MPa, which occurred as shown in Figure 2.6.3.7.

Through the above analysis, the maximum stress σ =110MPa was obtained, and took material safety factor as ςm=1, the yield limit of material Q345 was σs=345Mpa, the allowable stress was:

$$[\sigma] = \frac{\sigma_s}{\varsigma_m \varsigma_s} = 172.5MPa \tag{35}$$

$$\sigma = 110MPa < [\sigma] \tag{36}$$

The minimum fatigue safety factor of the pedestal was 1.4, which was satisfied with the analysis of stress and life.

The design life of the loading bracket was 50000000 times, and of stress and life distribution was shown in the figure below.

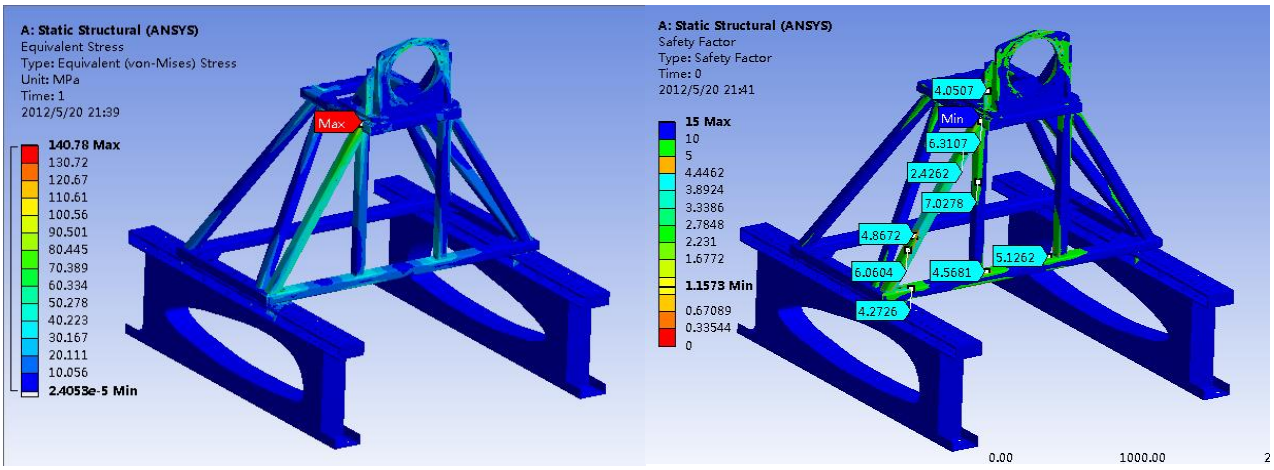

(a) Stress distribution (b) Life analysis

Fig. 6 Fatigue stress distribution and life analysis of supports

From the above figure, the stress concentration occurred locally in the loading bracket, and the maximum stress was 140MPa, and the maximum stress at the weld was 113.75 MPa which was measured by the stress probe.

Through the above analysis, the maximum stress σ =140MPa was obtained. The material safety factor was ςm=1, and the yield limit of material Q345 was σs=345Mpa, then the allowable stress was:

ISSN: 2414-1895 DOI: 10.6919/ICJE.202108_7(8).0037

$$[\sigma] = \frac{\sigma_s}{\varsigma_m \varsigma_s} = 172.5MPa \tag{37}$$

$$\sigma = 140MPa < [\sigma] \tag{38}$$

The maximum stress at the weld was σw=113.75MPa. The safety factor of the weld was ς_w=1.5, and the yield limit of material Q345 was σs=345Mpa, then the allowable stress was:

$$[\sigma] = \frac{\sigma_s}{\varsigma_w \varsigma_s} = 115MPa \tag{39}$$

$$\sigma = 113.75MPa < [\sigma] \tag{40}$$

The local life safety factor of the bracket was above 2.

5. Conclusion

According to the fatigue loading test of wind turbine blades, the vibration loading characteristics and loading equipment of the blade were studied, the following conclusions were drawn:

1. A set of fatigue excitation equipment of wind power blade driven by eccentric rotating mass was designed, which can meet the fatigue resistance test of wind power blades.

2. The start-stop and steady-state analysis of the exciting equipment was completed by using the law of conservation of energy and the theory of vibration, and the key parameters matching of the exciting equipment were completed.

3. The strength, deformation and fatigue life analysis of the key components (eccentric block, axle sleeve, pedestal and bracket) of the excitation equipment were carried out by using the finite element method, which verified the feasibility of the equipment used in fatigue loading test.

References

[1] DAI Ju-chuan, Yang Xin, Li Wen. Development of wind power industry in China: A comprehensive assessment[J]. Renewable and Sustainable Energy Reviews, 2018,156-164.

[2] CHEN Xiao, ZHAO Wei, ZHAO Xiao -lu, etal. Failure Test and Finite Element Simulation of a Large Wind Turbine Composite Blade under Static Loading[J]. Energy, 2014, 7, 2274-2297.

[3] SHI Ke-zhong, ZHAO Xiao-lu, XU Jian-zhong. Research on fatigue test of large horizontal axis wind turbine blade[J]. Acta energiae solaris sinica,2011,32(8):1264-1268.

[4] LIU De-shun, DAI Ju-chuan, HU Yan-ping, etal. Status and development trends of modern large-scale wind turbines[J]. China Mechanical Engineering, 2013,24(1):125-135.

[5] WHITE D, MUSIAL W, EEGBERG S. Evaluation of the NEW B-REX Fatigue Testing System for Multi-megawatt Wind Turbine Blades[J]. 43rd AIAA Aerospace Sciences Meeting and Exhibit, USA, 2005, 6:10-13.

[6] LIAO Gao-hua, WU Jian-zhong, WANG Yi-chun. System property analysis on chordwise fatigue loading for wind turbine blades[J].Chinses journal of construction machinery, 2014,12(5):450-453.